 FDMP, vol.1, no.3, pp.213-234, 2005

Coalescence and Non-coalescence Phenomena in Multi-material Problems and Dispersed Multiphase Flows: Part 2, A Critical Review of CFD Approaches

Marcello Lappa [1]

Abstract: The physical properties of many emulsions and metal alloys strongly depend on the multiphase morphology which is controlled to a great degree by particle-particle interaction during the related processing. In the present article significant effort is devoted to illustrate the philosophy of modeling for these phenomena and some insights into the physics. Within such a context working numerical techniques that have enjoyed a widespread use over recent years are presented and/or reviewed. Finally a focused and critical comparison of these possible approaches is reported illustrating advantages and disadvantages, strengths and weaknesses, past history and future directions.

1 Introduction

Currently many of the effects described in the first part of this work can be simulated in terms of direct numerical solution of the Navier-Stokes and energy equations in their complete nonlinear, viscous and coupled form. This has been made possible by the recent developments of moving-boundary methods.

Several techniques exist for tracking immiscible interfaces, each with its own strengths and weaknesses.

Along these lines the reader should be informed of the fact that from a general point of view, two broad strategies exist to deal with interface calculations. One (multiple-region formulation) is to use deformable meshes based on a finite volume or finite-element representation or body-fitted coordinates. The body-fitted coordinates approach, for instance, consists first of casting the flow equations, together with the free surface equations, into a curvilinear coordinate system, more convenient for numerical computations, and then of moving the grid points (on the free surface and in the total or part of the fluid domain) to fit the new free surface shape.

[1] MARS (Microgravity Advanced Research and Support Center), Via Gianturco 31 - 80146, Napoli, Italy, E-mail: marlappa@marscenter.it, marlappa@unina.it

The other strategy is to keep the mesh fixed (a uniform structured mesh with fixed topology), and to use a separate procedure to describe the position of the interface (single-region formulation). From this perspective, the main advantage offered by fixed uniform grids is the great simplicity they afford in the treatment of the bulk fluid regions, away from the interfaces. A further advantage of fixed-grid methods is to avoid the remeshing that may be necessary whenever interface motion deforms the grid exceedingly.

All these techniques can be re-classified under three main categories according to the intrinsic nature of the philosophy used to define their main features: capturing (also known as moving grid or Lagrangian approach), tracking (also known as fixed grid or Eulerian approach) and combined "hybrid" techniques. Capturing methods include marker particle (MP) schemes, body-fitted strategies, and the aforementioned (see Part 1) boundary integral method (BIM). In turn, tracking methods can be divided into two main approaches: surface tracking and volume tracking, which include pure Eulerian techniques, i.e. volume-of-fluid (VOF) and (implicit front tracking) level-set methods, and explicit hybrid front-tracking (also known as "immersed boundary" algorithm).

Amongst these, an indicator function is used which is a volume fraction (color function) for VOF methods or a level set for level-set methods. The indicator function is a scalar step function ϕ representing the space occupied by one of the fluids in the first case, and a smooth arbitrary function encompassing a prespecified isosurface which identifies the interface in the second case. The VOF method is widely adopted by in-house codes and built-in in commercial codes. It is a popular volume tracking algorithm that has proven to be a useful and robust tool since its development decades ago. Recently, level-set methods, originally introduced by Osher and Sethian (1988), have been applied to a wide variety of immiscible interfacial problems. These methods use a level function φ, with the 0 contour level defining the material inter-

face, much the same as the fractional volume function ϕ in the VOF method, to indicate the shortest distance to the interface.

Sections 2 and 3 provide a quite exhaustive picture of the state-of-the-art. Finally Sect. 4 is focused on a critical comparison of these methods illustrating advantages and disadvantages, strengths and weaknesses.

2 VOF - Volume of Fluid Method

Historically, pioneering work on the VOF (Volume of Fluid or Volume of Fraction, also known as Volume Tracking) methods goes back to Noh and Woodward (1976), but with Hirt and Nichols (1981a) and their SOLA-VOF code, the method became widely used.

As discussed by Rider and Kothe (1998), however, these techniques still possess solution algorithms that are too often perceived to be heuristic and without adequate mathematical formalism. Part of this misconception lies in the difficulty of applying standard hyperbolic PDE (partial differential equations) numerical analysis tools, which assume algebraic formulations, to methods that are largely geometric in nature (hence, the more appropriate term *volume tracking*). To some extent the lack of formalism in volume-tracking methods, manifested as an obscure underlying methodology, has impeded progress in evolutionary algorithmic improvements and application in particular to the case of immiscible metal alloys and emulsions (rare efforts are due to Iwasaki et al., 2001; Tang et al., 2004).

Despite some results being available for the case of rising and interacting bubbles (Esmaeeli and Tryggvason, 1998, 1999), in fact, the numerical simulation of these aspects in the case of drops sedimenting due to gravity or migrating owing to Marangoni forces can still be regarded as an open task. Despite the widespread use of these methods, VOF-based simulations dealing with these particular aspects are still very rare in the literature (rare and excellent efforts have been provided by Gueyffier et al. 1999; Mehdi-Nejad et al. 2003 for the case of droplet sedimentation; and Haj-Hariri et al., 1997 for the case of Marangoni migration).

The present section is devoted to the discussion of a general-purpose VOF method able to deal with particle (drop or bubble) motion due to gravity effects as well as with the Marangoni-migration phenomena (or both cases). In the light of the above discussion particular care is devoted to the formalism.

2.1 The variable material properties approach

The classical VOF formulation (see the excellent overviews of Rudman, 1997a; Rider and Kothe, 1998; Scardovelli and Zaleski, 1999; Kothe, 1999; Benson, 2002) relies on the fact that the two or more fluids (phases) are not interpenetrating. For each additional phase added to the model a variable is introduced: the volume fraction of the phase in the computational cell. In each control volume (computational cell), the volume fractions of all phases must sum to an unity. The fields for all variables and properties are shared by the phases and represent volume-averaged values, as long as the volume fraction of each of the phases is known at each location. Thus the variables and properties in any given cell are either purely representative of one of the phases, or representative of a mixture of the phases depending upon the volume fraction values. Hereafter, for the sake of simplicity only two immiscible phases are considered.

If the volume fraction of phase (1) in the cell is denoted as ϕ, the following three conditions are possible:

$$\begin{aligned} &\phi = 0 \quad \text{(the cell is empty of fluid (1))} \\ &\phi = 1 \quad \text{(the cell is full of fluid (1))} \\ &0 < \phi < 1 \quad \text{(the cell contains the interface)} \end{aligned} \tag{1}$$

Based on the local values of ϕ, the appropriate properties and variables are assigned to each control volume within the computational domain. If χ denotes the generic fluid property (e.g., density ρ, dynamic viscosity μ, thermal conductivity λ, specific heat coefficient C_p, etc.) the corresponding value in each cell is given by:

$$\chi = \chi_1 \phi + \chi_2 (1 - \phi) \tag{2}$$

which means that the concept of mixed properties is used to interpret the cells containing multiple fluids.

Accordingly, a single momentum equation is solved throughout the domain and the resulting velocity field is shared among the phases, i.e. the governing equations are written for the whole computational domain and the different phases are treated as a single fluid with variable material properties:

$$\underline{\nabla} \cdot \underline{V} = 0 \tag{3}$$

$$\frac{\partial(\rho\underline{V})}{\partial t} = -\underline{\nabla}p - \underline{\nabla}\cdot[\rho\underline{V}\underline{V}] + \underline{\nabla}\cdot\left[\mu\left(\underline{\nabla V} + \underline{\nabla V}^T\right)\right] + \underline{F}_g + \underline{F}_\sigma \quad (4)$$

$$\frac{\partial \rho C_P T}{\partial t} = [-\underline{\nabla}\cdot(\rho C_P \underline{V} T) + \underline{\nabla}\cdot(\lambda\underline{\nabla}T)] \quad (5)$$

where the source terms in eq. (4) take into account gravity ($\underline{F}_g$) and surface-tension ($\underline{F}_\sigma$) effects, respectively.

The phase variable is advected according to a simple transport equation:

$$\frac{D\phi}{Dt} = \frac{\partial\phi}{\partial t} + \underline{V}\cdot\underline{\nabla}\phi = 0 \quad (6)$$

The interfaces are tracked in volume-tracking methods by evolving fluid volumes forward in time with solutions of the above advection equation.

Since at any time in the solution, exact interface locations are not known (i.e. a given distribution of volume data does not guarantee a unique interface), interface geometry must be inferred, based on local volume data and the assumptions of a particular algorithm, before interfaces can be reconstructed. The reconstructed interface is then used to compute the volume fluxes necessary to integrate the volume-evolution equation (6), i.e. for for better computation of the convective contributions related to $\underline{V}\cdot\underline{\nabla}\phi$ (these aspects are discussed in Sect. 2.3).

This approach is referred to as single-region formulation since there is no need (from a computational point of view) to distinguish the different phases, i.e. to use different computational domains (this is the great advantage offered by such formulations).

2.2 The continuum surface force and stress models

With the Continuum Surface Force (CSF) model proposed for the first time by Brackbill et al. (1992), the addition of surface-tension effects to the VOF calculation results in a source term in the momentum equation, i.e. $\underline{F}_\sigma$ in eq. (4).

In practice, the well-known Young-Laplace equation can help the reader to understand the origin of such a source term. Consider, for instance, the case where the surface tension is constant along the surface and where only the forces normal to the interface are present (according to the theoretical arguments pointed out in Part 1 this special case occurs if isothermal conditions are considered and/or the liquid is compositionally homogeneous). The pressure jump across the surface depends on the surface-tension coefficient σ and the surface curvature as measured by two radii in orthogonal directions R_1 and R_2:

$$p_2 - p_1 = \sigma\left(\frac{1}{R_1} + \frac{1}{R_2}\right) \quad (7a)$$

$$\text{i.e. } \Delta p = \sigma K \quad (7b)$$

where K is the curvature.

In the light of the foregoing arguments, the surface tension can be written simply in terms of a pressure jump across the surface. This force in turn can be expressed as a volume force in eq. (4) using the divergence theorem or a similar artifice to replace the surface force with a volume force. The end of the story is that the interfacial surface forces can be incorporated as body forces per unit volume in the momentum equations rather than as boundary conditions. Instead of a surface-tensile-force boundary condition applied at a discontinuous interface of the two fluids, a volume force can be used that acts on fluid elements lying within a transition region of finite thickness. This also means that the CSF formulation makes use of the approach that discontinuities can be approximated, without increasing the overall error of approximation, as continuous transitions within which the fluid properties vary smoothly from one fluid to the other over a distance of O(h), where h is a length comparable to the resolution of the computational mesh. Surface tension, therefore, is felt everywhere within the transition region through the volume force included in the momentum equations. A similar mathematical treatment is possible for the contribution related to surface-tension gradients along the interface (Marangoni stress).

It is known, in fact, that the expression for the stress jump $\underline{f}$, across the interface is given by (see the elegant formalism of Haj-Hariri et al., 1997)

$$\underline{f} = \left[\sigma K\underline{\hat{n}} - \frac{\partial\sigma}{\partial T}\left(\underline{\underline{I}} - \underline{\hat{n}}\underline{\hat{n}}\right)\cdot\underline{\nabla}T\right] \quad (8)$$

where $\underline{\hat{n}}$ is the unit vector perpendicular to the fluid/fluid interface, K is the curvature and $\underline{\underline{I}}$ is the identity matrix:

$$\underline{\hat{n}} = \frac{\underline{\nabla}\phi}{|\underline{\nabla}\phi|} \quad (9)$$

$$K = -\underline{\nabla}\cdot\underline{\hat{n}} = \frac{1}{|\underline{n}|}\left[\frac{\underline{n}}{|\underline{n}|}\cdot\underline{\nabla}|\underline{n}| - \underline{\nabla}\cdot\underline{n}\right] \quad (10)$$

K is formally a second derivative of ϕ, but it is usually computed according to eq. (10) since direct discretization of second and higher derivatives can lead to major inaccuracies for low-order methods, and becomes rather complicated at high order.

The surface force per unit interfacial area, should be added in the momentum equation as $\underline{f}\,\delta$ where δ is the Dirac-pulse function used to localize the force explicitly at the interface. Using some theoretical artifices (as previously discussed) it can formally be replaced by its volume-distributed counterpart, $\underline{F}$, which satisfies

$$\int_{-\infty}^{\infty} \underline{F}(s)ds = \int_{-\infty}^{\infty} \underline{f}(s)\delta(s)ds \tag{11}$$

where (s) is a level-set function denoting the normal distance from the interface (the interface corresponds to s=0) and δ(s) is the Dirac delta function with its singularity on the interface. Rigorously speaking, f is not defined for nonzero s and must be extended appropriately (e.g., it can be assigned a value of zero for nonzero s because of the presence of the delta function). A comparison of the two integrals in eq. (11) suggests $\underline{F}=\underline{f}\delta$(s). Although this expression is of little value in its present form, much can be gained from it if a mollified delta function is used, consistent with the smearing of the interface. Recognizing that

$$\int_{-\infty}^{\infty} \delta(s)ds = \int_{-\infty}^{\infty} \underline{\hat{n}}\cdot\underline{\nabla}\phi ds = 1 \tag{12}$$

the mollified delta function can be defined as $|\underline{\nabla}\phi|$which, in turn, leads to $\underline{F}=\underline{f}|\underline{\nabla}\phi|$.

Thus the second source term in eq. (4) reads:

$$\underline{F}_\sigma = \left[\sigma K\underline{\hat{n}} - \frac{\partial\sigma}{\partial T}\left(\underline{\underline{I}} - \underline{\hat{n}\hat{n}}\right)\cdot\underline{\nabla}T\right]|\underline{\nabla}\phi| \tag{13}$$

where, as previously discussed in the light of the Young-Laplace equation, the first term in the square parentheses is the normal stress contribution responsible for the shape equilibrium in the perpendicular direction, whereas the second is the thermal Marangoni shear stress along the surface that can be responsible for the Marangoni migration phenomena (solutal effects are not considered in the present work).

It is important to highlight how a reliable computation of both K and $\underline{\hat{n}}$ is not easy and special care must be devoted to such computation. Usually the unit normal-vector results from the gradient of a smoothed phase field ϕ (the so-called mollification).

The smoothed VOF function can be computed for instance by convolving ϕ with a B-spline of degree l (Brackbill et al., 1992). Such a procedure may be applied iteratively by multiple passes through the mesh for increased degrees of smoothing.

For further details on these aspects see, e.g., the excellent works of Rider and Kothe (1998), Guyeffier et al. (1999) and Williams et al. (1999a,b) who worked to improve the accuracy of the VOF geometrical information using convolution.

To summarize:

$$\underline{F}_\sigma = \left[\sigma K\underline{\hat{n}} - \frac{\partial\sigma}{\partial T}\left(\underline{\underline{I}} - \underline{\hat{n}\hat{n}}\right)\cdot\underline{\nabla}T\right]|\underline{\nabla}\hat{\phi}| \tag{14}$$

where $\hat{\phi}$ is the mollified phase-field variable.

The treatment of the source term $\underline{F}_g$ taking into account gravity is relatively simple if compared with the corresponding effort provided for the modeling of $\underline{F}_\sigma$.

In fact, the first source term in eq. (4) simply reads:

$$\underline{F}_g = -\rho\underline{g} = -\left(\rho_1\phi + \rho_2(1-\phi)\right)\underline{g} \tag{15a}$$

and since, according to the Boussinesq hypothesis (where β_{Ti} is the thermal expansion coefficient and ρ_{io} is the density for $T = T_o$)

$$\begin{aligned}\rho_i &= \rho_{i0}\left[1-\beta_{Ti}(T-T_o)\right] \rightarrow \\ \underline{F}_g &= -\rho\underline{g} = -\left[\rho_{1o}\phi + \rho_{2o}(1-\phi)\right]\underline{g} + \\ &\left[\rho_{1o}\beta_{T1}\phi + \rho_{2o}\beta_{T2}(1-\phi)\right](T-T_o)\,\underline{g}\end{aligned} \tag{15b}$$

where the first and the second terms in the square parentheses can be responsible for sedimentation owing to the different density of the phases (e.g., $\rho_{1o} > \rho_{2o}$) and for possible onset of buoyant convection (in nonisothermal conditions), respectively.

Gravity can manifest itself in the process of drop sedimentation (or bubble/light-drop rise), in fact, in two ways. It has a direct effect on the drop velocity, through buoyancy, and in a more subtle (but not necessarily insignificant) way through natural convection in the surrounding liquid. This convection can directly affect drop

motion and also alter the temperature gradients at the interface.

As anticipated, the main advantage of the above formulation is the topological simplification resulting from the incorporation of the interfacial jump conditions into the bulk equations. This eliminates the rather involved task of generating grids for the interior and exterior domains that must be tracked and reconstructed after each iteration step (the so-called multiple-region formulations). With the VOF formulation a single grid can be generated without regard for the actual shape of the moving interface. However, as anticipated in Sect. 2.1 a reconstruction technique is required. Different procedures can be used in principle to reconstruct the interface (see the next section).

2.3 Interface-reconstruction techniques

The ϕ-field is the only phase information stored in VOF methods. Approximate interface locations are found from a so-called interface reconstruction. This is needed, as anticipated, for advecting ϕ, for determining the local properties (density, viscosity, etc.) and for better graphical representation. In earlier versions, usually called SLIC (Simple Line Interface Construction Method) after Noh and Woodward (1976), interfaces were approximated with either a horizontal or vertical line in each cell. Certainly, such a reconstruction appears rather crude. Nevertheless, it has been used in many versions up to the present day, and many reasonable simulation results were obtained (see, e.g., Rudman, 1997b).

The SLIC method approximates interfaces as piecewise constant, where interfaces within each cell are assumed to be lines (or planes in three dimensions) aligned with one of the logical mesh coordinates. The Hirt-Nichols (h-n) scheme, as used in the Sola-Vof code (Nichols et al., 1980; Hirt and Nichols, 1981a,b), is a variation of the piecewise constant method (piecewise constant/"stair-stepped" approximation). In piecewise constant/stair-stepped methods, interfaces are also forced to align with mesh coordinates, but are additionally allowed to "stair-step" (align with more than one mesh coordinate) within each cell, depending upon the local distribution of discrete volume data.

A notable feature of the SLIC method is that its volume fluxes can be formulated algebraically, i.e., without needing an exact reconstructed interface position. The volume fluxes can be expressed as a weighted sum of upwind and downwind contributions, depending upon the orientation of the interface relative to the local flow direction. For this case interface reconstruction is used only for visualization purposes.

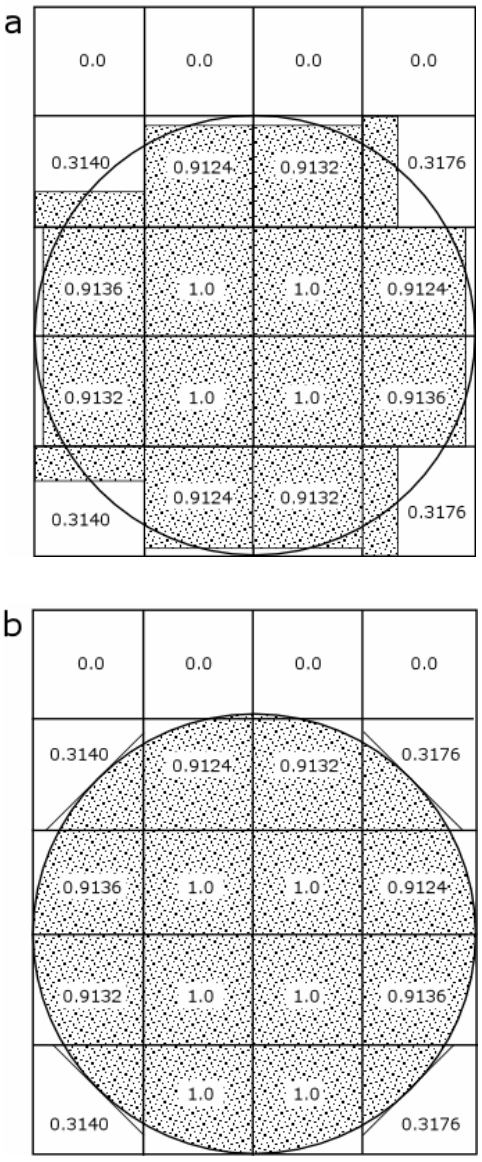

Figure 1 : Reconstructed interfaces (shaded regions) for a drop using the SLIC and PLIC methods. Numbers in the cells denote volume fractions. (a) SLIC reconstruction. (b) PLIC reconstruction.

More accurate reconstructions are possible with PLIC (Piecewise Linear Interface Construction, Youngs, 1982 and 1984; Ashgriz and Poo, 1991). The interface is approximated by a straight line of arbitrary orientation in

each cell. Its orientation is found from the liquid distribution in the neighbor cells; given the volume fraction of one of the two fluids in each computational cell and an estimate of the normal vector to the interface, a planar surface is constructed within the cell having the same normal and dividing the cell into two parts each of which contains the proper volume of one of the two fluids.

This has several advantages: the fluxes of ϕ, with which the phase field ϕ is updated, can be determined more accurately, and essentially free of numerical diffusion. Fluid properties can be allocated accurately. Finally the straight lines also give a graphical representation of good quality.

See the excellent overview of Rider and Kothe (1998) for additional details on these geometrical reconstruction techniques.

Figure 1 shows reconstructed interfaces (shaded regions) for a drop of arbitrary radius (continuous line) using the SLIC and PLIC methods.

More complex piecewise interface reconstructions have also been developed over recent years, e.g., piecewise circle (Mosso et al., 1997), piecewise parabolic (Renardy and Renardy, 2002), piecewise spline (Ginzburg and Wittum, 2001 and Lòpez et al., 2004), and interface reconstruction methods based on least squares fit (Scardovelli and Zaleski, 2003).

2.4 Discretization

The basic numerical algorithm for the solution of eqs. (3-5) is the well-known (see, e.g., Lappa, 2004) splitting method. For the case under investigation it must be modified to take into account the fact that two phases with different density are present in the computational domain; it consists of the following two steps (as an example, a first-order temporal integration scheme is used):

$$\underline{V}^* = \underline{V}^n + \Delta t \frac{1}{\rho^n}\left\{-\underline{\nabla}\cdot[\rho\underline{V}\underline{V}] + \underline{\nabla}\cdot\left[\mu\left(\underline{\nabla V} + \underline{\nabla V}^T\right)\right] + \underline{F}_g + \underline{F}_\sigma^t\right\}^n \tag{16}$$

where $\underline{F}_\sigma^t = \left[-\frac{\partial\sigma}{\partial T}\left(\underline{I} - \hat{n}\hat{n}\right)\cdot\underline{\nabla}T\right]|\underline{\nabla}\phi|$

$$\underline{V}^{n+1} = \underline{V}^* + \Delta t \frac{1}{\rho^n}\left[-\underline{\nabla}p + \underline{F}_\sigma^p\right]^n \tag{17}$$

where $\underline{F}_\sigma^p = [\sigma K\underline{\hat{n}}]\,|\underline{\nabla}\phi|$ and the elliptic equation reads:

$$\underline{\nabla}\cdot\left[\frac{1}{\rho}\underline{\nabla}p\right]^n = \frac{1}{\Delta t}\underline{\nabla}\cdot\underline{V}^* + \underline{\nabla}\cdot\left[\frac{1}{\rho}\underline{F}_\sigma^P\right]^n \tag{18}$$

During each time step, the intermediate velocity field V* is calculated from eq. (16), and used to obtain the pressure through an iterative solution of eq. (18). Subsequently, the new pressure distribution is used in eq. (17) to advance the velocity field to the next time step.

Once the new velocity field, V^{n+1}, is determined, The phase variable is advected according to eq. (6) and the interface-reconstruction technique used; this step provides the new distribution ϕ^{n+1}.

Then, the temperature field (if required) is updated by using explicit Euler time marching in eq. (19):

$$T^{n+1} = \frac{[\rho C_P T]^n + \Delta t\left[-\underline{\nabla}\cdot(\rho C_P\underline{V}T) + \underline{\nabla}\cdot(\lambda\underline{\nabla}T)\right]^n}{[\rho C_P]^{n+1}} \tag{19}$$

3 Level-set methods

3.1 General properties

As already outlined in the introduction, unlike the VOF methods, where the indicator function is a scalar step function ϕ representing the space occupied by one of the fluids, level-set techniques rely on a smooth arbitrary function encompassing a prespecified isosurface which identifies the interface. In practice, the method embeds the interface Γ bounding the region Ω occupied by one of the two fluids and separating the two phases in a domain of R^2(2D problem) or R^3 (3D problem) as the zero level set of a higher dimensional function $\varphi(\underline{r},t)$ i.e. $\Gamma(t) = \underline{r}|_{\varphi(\underline{r},t)=0}$. The level set function has the following properties:

$$\begin{aligned} &\varphi(\underline{r},t) > 0 \quad \text{for} \quad \underline{r} \notin \Omega \\ &\varphi(\underline{r},t) = 0 \quad \text{for} \quad \underline{r} \in \partial\Omega = \Gamma(t) \\ &\varphi(\underline{r},t) < 0 \quad \text{for} \quad \underline{r} \in \Omega \end{aligned} \tag{20}$$

and in many circumstances it can be simply defined as the signed Euclidean distance to the interface.

Thus, the variable φ is responsible for capturing the interface in an implicit fashion at each moment in time (this also provides a simple explanation for the name of the level-set method: at any time t, the evolving curve corresponds to the locus of all points such that $\varphi(\underline{r},t)=0$, and

that locus is a level curve of the φ function). The locus of all points such that φ(r,t)=c, simply contours around the original curve, where c is an arbitrary positive or negative constant.

Intrinsic geometric properties of the front can be calculated directly from the level set function, including the unit normal to the interface

$$\hat{\underline{n}} = \frac{\underline{\nabla}\varphi}{|\underline{\nabla}\varphi|} \tag{21}$$

and the curvature

$$K = \underline{\nabla} \cdot \left(\frac{\underline{\nabla}\varphi}{|\underline{\nabla}\varphi|} \right) \tag{22}$$

This method, first introduced by Osher and Sethian (1988), is conceptually similar to a VOF model in that the movement of the interface is taken care of implicitly through an advection equation for φ. Unlike the VOF model, however, there is no arbitrary interface width introduced in the level-set method and, as a result, no interface-reconstruction techniques (e.g., PLIC) are required.

Its motion is analyzed by convecting the φ values (levels) with the velocity field $\underline{V}$:

$$\frac{D\varphi}{Dt} = \frac{\partial\varphi}{\partial t} + \underline{V} \cdot \underline{\nabla}\varphi = 0 \tag{23}$$

$\underline{V}$ being provided by the solution of the Navier-Stokes equations (3-5).

3.2 The heaviside function

Following Sussman et al. (1994) it is convenient to introduce the so-called heaviside function defined as:

$$\begin{aligned} H(\varphi) &= 0 \quad \text{if } \varphi < 0 \\ H(\varphi) &= 1 \quad \text{if } \varphi > 0 \end{aligned} \tag{24}$$

This function formally behaves as the volume of fraction ϕ introduced in Sect. 2.1. It plays an important role within the numerical framework related to level-set methods as it allows the treatment of variable fluid properties such as the density, the viscosity, etc., within the model of the variable material properties approach already introduced in Sect. 2.1, i.e.

$$\chi = \chi_{EXT} H + \chi_{INT}(1-H) \tag{25}$$

χ denoting the generic fluid property.

The heaviside function also allows a simple and efficient treatment of the interface source terms and, in particular, of the surface tension forces. Following the arguments elucidated in Sect. 2.2 (see, in particular, eqs. (11) and (12) and the related discussion), it is evident that a mollified delta function can be defined as $|\underline{\nabla}H|$.

Thus the second source term in eq. (4) can be written as:

$$\underline{F}_\sigma = \left[\sigma K \hat{\underline{n}} - \frac{\partial\sigma}{\partial T} \left(\underline{\underline{I}} - \hat{\underline{n}}\hat{\underline{n}} \right) \cdot \underline{\nabla} T \right] |\underline{\nabla}H| \tag{26}$$

that, since from a formal point of view

$$\underline{\nabla}H = \frac{dH}{d\varphi}\underline{\nabla}\varphi \tag{27}$$

can be rewritten as:

$$\underline{F}_\sigma = \left[\sigma K \hat{\underline{n}} - \frac{\partial\sigma}{\partial T} \left(\underline{\underline{I}} - \hat{\underline{n}}\hat{\underline{n}} \right) \cdot \underline{\nabla} T \right] \frac{dH}{d\varphi} |\underline{\nabla}\varphi| \tag{28}$$

Although this expression is of little value in its present form, much can be gained from it if a mollified heaviside function is used (see the discussions in Sect. 3.3).

3.3 The narrow band approach

The basic level-set method concerns a function φ(r,t) that is defined throughout space. Clearly this is useless if one only cares about information near the zero level-set. In practice, eq. (23) can be solved in a neighborhood of $\Gamma(t)$ of width $m\Delta r$=ε, where m is typically 5 or 6. Points outside this neighborhood need not to be updated by this motion. This strategy is also known as the "narrow band approach" (Adalsteinsson and Sethian, 1995). A strip centered on Γ is built around the interface, with a user-prescribed width (the optimal width m for a specific problem depends on the quantities involved). Since, as explained before, in many cases φ(r,t) is assumed close to a signed distance function, the narrow band can be simply defined by locating the points using the following criterion:

$$\underline{r}\big|_{|\varphi(\underline{r},t)|<\varepsilon} \tag{29}$$

in the narrow band, the heaviside function is usually mollified according to eq. (30) given below:

$$H(\varphi) = \begin{cases} 0 & \text{if } \varphi < -\varepsilon \\ \frac{1}{2}\left[1 + \frac{\varphi}{\varepsilon} + \frac{1}{\pi}\sin\left(\frac{\pi\varphi}{\varepsilon}\right)\right] & \text{if } -\varepsilon \le \varphi \le \varepsilon \\ 1 & \text{if } \varphi > \varepsilon \end{cases}$$

(30)

that gives $\frac{dH}{d\varphi} = \frac{1}{2\varepsilon}\left[1+\cos(\frac{\pi\varphi}{\varepsilon})\right]$ for $-\varepsilon < \varphi < \varepsilon$ and zero elsewhere, allowing the extension of the continuum surface force and stress models described in Sect. 2.2 to the level-set methods. Other alternatives to the smoothed delta and heaviside functions with possible better convergence properties have recently been analyzed by Tornberg and Engquist (2004).

3.4 The redistancing algorithm

After solving eq. (23) for one time step, the level-set function will no longer be equal to the distance away from the interface. It is necessary to *reinitialize* φ to be a signed distance function. Re-initialization at some moment of time t can be regarded as the process of replacing the current level set function $\varphi(\underline{r},t)$ by another function $\varphi^{reinit}(\underline{r},t)$ that has the same zero contour but is better behaved and becomes the new level set function to be used as initial data until the next re-initialization.

In practice, re-initialization of the level set function φ as a signed distance to the interface is needed in two cases: first, steep or flat gradients can develop that will in turn affect the estimation of the geometrical properties of the interface via eqs. (21) and (22); second, if a "narrow band" type method is used, then the level set function must be re-initialized to a signed distance function each time the "narrow band" is rebuilt. Chopp was the first to recognize the need for reinitialization (Chopp, 1993, Hogea et al., 2005).

This step can be accomplished (Peng et al., 1999, Sussman and Fatemi, 1999) by solving

$$\begin{aligned} &\frac{\partial \psi}{\partial \tau} + sgn(\varphi)\left[|\underline{\nabla}\psi| - 1\right] = 0 \\ &\psi(\underline{r},0) = \varphi(\underline{r},t) \end{aligned} \tag{31}$$

where τ is a fictious pseudo-time for relaxing the equation to steady-state at a fixed real time t. Following Osher and Fedkiw (2002), in order to define the distance φ in a band of width ε around $\Gamma(t)$, eq. (31) should be solved only for $\tau = O(\varepsilon)$.

The sign function can be computed as

$$sgn(\varphi) = 2H(\varphi) - 1 \tag{32}$$

In practice, in order to ensure the necessary accuracy of the curvature and to enhance volume conservation during redistancing, the sign function is usually mollified as proposed in Peng et al. (1999):

$$sgn(\varphi) = \frac{\varphi}{\sqrt{\varphi^2 + h^2}} \tag{33}$$

where h represents the size of the fixed Cartesian mesh chosen to discretize the problem (i.e Δr).

The function φ being reinitialized to be signed distance to $\Gamma(t)$ only near the boundary, (solving eq. (23) only locally near the interface $\Gamma(t)$), the complexity of this calculation is lowered by an order of magnitude (Osher and Fedkiw, 2001, 2002). The operation count in three dimensions for N^3 grid points, in fact, drops to $O(mN^2)$, providing a significant cost reduction. This makes the cost of level-set methods competitive with other techniques. For additional information on these techniques and related variants, the reader may consider the excellent articles of Sethian (1995, 1996, 1999a,b, 2001), Sussman and Smereka (1997), Sethian and Smereka (2003), the variational approaches of Zhao et al. (1996, 1998).

4 Critical comparison of different moving boundary strategies

In this section ancient and modern moving boundary methods are reviewed and discussed showing analogies and differences. Emphasis is given to possible advantages and limitations, potentialities and drawbacks to provide the reader with a brief but clear picture of the past evolutionary progress as well as of the current state of the art.

4.1 Front capturing methods

The first method capable of modeling multiphase flow, separated by a moving interface, was the Marker and Cell (MAC) of Harlow and Welch (1965).

This method can be regarded as a combination of a Eulerian solution of the basic flow field, with Lagrangian marker particles attached to one phase to distinguish it from the other phase. In practice, it uses particles with no mass nor energy, distributed in the whole fluid volume to trace the free surface. Those massless particles are fictitious, of Lagrangian type, play no role in the dynamics of the fluid and are not accounted for in the solution of the flow governing equations. Initially distributed in the whole fluid volume, they are moved passively with the

local fluid velocity. The instantaneous surface configuration, can be determined by finding the markers' position after advection.

The computational procedure is very simple and consists of two main steps:

1. the governing equations of the flow are solved on a fixed computational grid and the velocity field is determined inside the fluid domain.

2. each particle is moved according to the velocity at its position.

With these techniques, small initial errors quickly become compounded, and awkward subjective methods must be used to add or remove marker points as they get too far apart or too close together.

More accurate and modern variants have been proposed over recent years with marker points planted along the surface and followed during their motion (Tomè and McKee, 1994; Chen et al., 1995; Lapenta and Brackbill, 1994; Raad et al., 1995; Rider and Kothe, 1995b; Chen et al., 1997; Torres and Brackbill, 2000).

However, like many other simpler approaches to modeling propagating interfaces, the marker-point methods (MP) fail in modeling some of the more complex motions of a surface. In flows with interface stretching and tearing, for instance, regions which lack a sufficient number of particles tend to be formed (this problem was also observed in earlier methods based on the seeding of particles everywhere in the computational domain, e.g., Harlow and Welch, 1965). As a consequence, in order to accurately resolve the interface for all time, these methods need to periodically readapt the particle distribution to the deformed interface (this idea of adding and deleting particles has been addressed by many authors, see for example Lapenta and Brackbill, 1994).

Furthermore, the storage requirement is significantly high since a very large number of point coordinates must be stored in addition to the bulk flow grid points. Moreover, even with a large number of markers, it is difficult to determine the orientation of the surface in a computational cell.

For these reasons MP methods have been rarely used in the literature.

With boundary-integral methods, similarly, only a discretization of the interfaces is necessary since the evolution of a deformable drop (or bubble) is described by time integrating the fluid velocity on a set of N interfacial marker points; marker point velocities are obtained by solving a second-kind boundary-integral equation over the surfaces. In practice, in these methods the flow equations are mapped from the immiscible fluid domains to the sharp interfaces separating them thus reducing the dimensionality of the problem (the computational mesh discretizes only the interface, for the state-of-the-art see, e.g., Pozrikidis, 1992, Zinchenko et al., 1997; 1999; Cristini et al., 2001; Hou et al., 2001; and Bazhlekov et al., 2004).

Along these lines, Hooper et al. (2001) developed a novel 3D adaptive remeshing algorithm for multiphase flows based on the finite element method (FEM). It should be pointed out, however, that in finite element methods, the fluid domains are discretized by a volume mesh and thus the dimensionality is not reduced. Both these approaches (BIM and FEM) lead to accurate and efficient solution of the flow equations because the interface is part of the computational mesh and the equations and interface boundary conditions are posed exactly.

The limits of the boundary-integral approach have been already outlined in the first part of this work (Lappa, 2005b); they are often limited to the case of very viscous flows and "close" interaction of particles.

4.2 The front tracking method

Another important category of moving boundary methods is represented by the so-called "front tracking".

This strategy can be regarded as a hybrid between a front capturing and a volume tracking technique. A stationary regular grid, in fact, is used for the fluid flow, but the interface is tracked by a separate unstructured grid of lower dimension than that used for the conservation equations (in practice, like in the MP approach, the fluid boundary is resolved by discrete computational Lagrangian points that are moved by interpolating their velocity from the underlying Eulerian grid). This cluster of points is usually referred to as the "front". It is used to keep the density and viscosity stratification sharp and to calculate surface tension forces. The algorithm foresees that at each time step information is passed between the front and the stationary grid.

Unlike multiple-region methods where each phase is treated separately, all phases are still treated together by solving a single set of governing equations for the whole flow field. In practice, this means that the single-region

formulation used is common to other techniques for multifluid flows such as the VOF (Volume of Fluid) and level-set methods.

It is worthwhile to recall, however, that in these methods the phase boundary is not tracked explicitly, but reconstructed from an indicator function, as illustrated in Sects. 2 and 3. Explicitly tracking the interface in the front tracking method avoids the difficulty of advecting such a function and allows accurate evaluation of surface forces. This method was introduced by Unverdi & Tryggvason (1992a,b); various improvements have been proposed over recent years (e.g., Popinet and Zaleski, 1999; Tryggvason et al., 2001).

Despite a lack of explicit enforcement of volume conservation, front tracking methods are quite successful in conserving mass since they seem to preserve material characteristics for a long time. However, it is well known that they pose many difficulties in the reconstruction of the interface especially in three spatial dimensions for pinching and merging droplets (Tryggvason et al., 2001).

As the front moves, it deforms and stretches. The resolution of some parts of the front can become inadequate, while other parts become crowded with front elements. To maintain accuracy, additional elements must either be added when the separation of points becomes too large or the points must be redistributed to maintain adequate resolution. This is a typical problem of Lagrangian approaches as already illustrated for the MP methods. The markers need to be continually redistributed because their distribution varies with time due to velocity gradients and it is therefore necessary to redistribute the markers evenly in all fluid cells when they tend to spread disproportionally.

Superimposed on this is the problem related to topology changes.

In general, numerical simulations of multiphase flow must account for topology changes of the phase boundary when, for example, drops or bubbles break up or coalesce. When the interface is explicitly tracked by connected marker points as in the front tracking approach, such changes must be accounted for by changing the connectivity of the points in the appropriate way. The complexity of this operation is often cited as the greatest disadvantages of front tracking methods. If the characteristics in a given region merge (e.g., if two droplets coalesce), marker points must be deleted.

Accomplishing topology changes in a front tracking code is generally a two step process. First, the part of the front that should undergo topology change must be identified and then the actual change must be done. Rupture or coalescence can take place anywhere and it is necessary to search the whole front to find where two fronts or two parts of the same front are close to each other. The simplest but least efficient way to conduct this search is to compute the distance between the centroids of every front elements. By dividing the computational domain into small sub regions and sorting the front elements according to location, this operation can be made reasonably efficient. This does, however, add to the complexity of the code and make these methods quite cumbersome.

Recently, Shin and Juric (2002) have presented a variant that seems to overcome many of these problems. The method is designed so that the phase surface is treated as a collection of physically linked but not logically connected surface elements. Eliminating the need to book keep logical connections between neighboring surface elements greatly simplifies the Lagrangian tracking of interfaces, particularly for 3D flows exhibiting topology change. Three-dimensional simulations of bubble merging and droplet collision, coalescence, and breakup have clearly demonstrated the new method's ability to easily handle topology change by film rupture or filamentary breakup.

4.3 Eulerian approaches

VOF and level-set methods do not require mesh cut-and-connect operations because the mesh elements do not lay on the interface, but rather the interface evolves through the mesh (Cristini and Tan, 2004). The fluid discontinuities (*e.g.*,density, viscosity) are smoothed and the surface tension force is distributed over a thin layer near the interface to become a volume force (surface tension being the limit as the layer approaches zero thickness, as illustrated in Sects. 2 and 3).

These methods, have had varying degrees of success correctly modeling multiphase flows with large vortical components.

In order to compare the fidelity of these schemes, Rider and Kothe proposed a set of test problems (1995a, 1998) which approximate flows with large vortical components. In a comparison of various Lagrangian and Eulerian algorithms for these flows, they found that Lagrangian tracking schemes maintain filamentary interface struc-

tures better than their Eulerian counterparts. In the same study, it was noted that when fluid filaments become too thin to be adequately resolved on the grid, level-set methods lose (or gain) mass while VOF SLIC methods form "blobby" filaments to locally enforce mass conservation (Lafaurie et al., 1994).

These bobbly structures correspond to the unphysical creation of what Noh and Woodward (1976) termed *flotsam* ("floating wreckage") and *jetsam* ("jettisoned goods"). These terms are appropriate for isolated, submesh-size material bodies that separate from the main material body because of errors induced by the volume tracking algorithm. These material remnants tend to be ejected from interfaces in piecewise constant volume tracking methods when the flow has significant vorticity and/or shear near the interface. The presence of flotsam near interfaces can severely compromise the overall interfacial flow solution, especially when interface dynamics (e.g., surface tension and phase change) are also being modeled.

Modern VOF methods, however, have solved many of these problems (e.g., Pilliod and Puckett, 1997; Puckett et al., 1997; Rudman, 1998; Williams et al., 1999a,b; Scardovelli and Zaleski, 2000; Harvie and Fletcher, 2000 and 2001; Renardy et al., 2001). More accurate VOF techniques (PLIC and more recent variants) do not produce isolated small fluid bodies (flotsam) which appear in VOF/SLIC techniques even for simple flows (detailed comparisons of numerical inaccuracies related to the different VOF variants have been reviewed by Kothe and Rider, 1995 and Ccerne et al., 2002).

In particular, Aulisa et al. (2003a) have presented recently a new class of algorithms that preserve mass exactly on a Cartesian mesh. They demonstrated that exact mass conservation is possible and that there are no undershoots or overshoots of the volume fraction which always remains constrained between zero and one.

As anticipated, in contrast to modern VOF techniques and the hybrid front tracking method of Tryggvason and coworkers (both have proven to conserve mass very accurately), a well-known drawback of the level-set method is mass loss/gain, i.e. the mass (or volume for incompressible flows) of the fluid is not conserved. Even though the zero level sets of φ can remain unchanged with some order of accuracy during the redistancing, the volume enclosed by the zero level sets is not conserved as φ evolves according to eq. (23). This leads, for instance, to a mass error in the simulation of drop coalescence.

Attempts to improve mass conservation in level-set methods have led to a variety of reinitialization variants, from the original redistancing algorithm of Sussman et al.(1994) to a more recent method by Sussman et al. (1998) and Sussman and Fatemi (1999) that constrains the reinitialization scheme to approximately conserve area (volume).

Despite these problem, however, level-set methods offer important geometrical advantages. A drawback of the VOF, in fact, is that it is hard to compute accurate interface normals and curvatures because of the discontinuity in ϕ (the reconstructed interface is not smooth or even continuous, lowering the accuracy of the geometrical information). Since φ is continuous, the calculation of the interface normal and curvature in the level-set approach is natural, easy and accurate, in contrast to the corresponding calculations in the VOF method, that require unphysical smoothing of ϕ as pointed out in Sect. 2.2.

There are also other limitations in the VOF approach. The proper use of these models also requires, as explained in Sect. 2.3, that an asymptotic analysis is performed in order to obtain a mapping between the function ϕ and the sharp-interface, i.e. a very accurate interface-reconstruction technique is required (e.g., the PLIC technique). Moreover, computationally, the grid spacing must be small enough to resolve the interfacial region. The interface is, in fact, defined by the condition $0 < \phi < 1$ and is, therefore, associated with a somewhat arbitrary thickness (the width depends on the resolution of the computational mesh).

These reconstruction procedures are very laborious and not easy to implement. On the contrary, the level-set computational approach has the capability to track the motion of the interface without resorting to mathematical manipulations and complex reconstruction techniques. Also, shape changes, corner and cusp development, topological merging and breaking are naturally obtained in this setting without elaborated machinery or failure (see Chang et al., 1996).

4.4 Other hybrid variants

In the light of the discussion in the foregoing sections, it is evident that each algorithm has readily identifiable strengths and weaknesses, which, if understood and

quantified, could result in a hybrid, unified algorithm possessing the strengths of many different strategies.

Sussman and Puckett (2000) were the first to combine the VOF and level-set techniques (CLSVOF) in order to alleviate some of the geometrical problems of the VOF method and some of the mass-loss problems of the level-set technique (see also Sussman, 2003, and Jimènez et al., 2005). The underlying philosophy is discussed below.

With the CLSVOF approach, both ϕ and φ are tracked according to eqs. (6) and (23), respectively. The level-set function φ is used to calculate the unit normal and curvature of the interface; ϕ together with the unit normal calculated from φ, is used to reconstruct the new interface (e.g., by a PLIC technique, thus enforcing mass conservation). Finally, φ is reset to a signed distance function based on the reconstructed interface. By this combined strategy, volume can be conserved very accurately (the tracking of ϕ is essential for enforcing mass conservation) and the computation of geometrical parameters becomes very accurate (since φ is continuous).

Recently, other methods that couple two different schemes have been developed. Examples are the mixed markers and VOF method (Aulisa et al., 2003b) and the mixed markers and level-set method (Enright et al., 2002).

In particular the technique proposed by Enright et al. (2002) seems to be very promising as it combines the best properties of an Eulerian level-set method and a marker particle Lagrangian scheme. Such method randomly places a set of marker particles near the interface (defined by the zero level set) and allows them to passively advect with the flow. Since in fluid flows, particles do not cross the interface except when the interface capturing scheme fails to accurately identify the interface location, if the marker particles initially seeded on one side of the interface are detected on the opposite side, this indicates an error in the level set representation of the interface. The method fixes these errors by locally rebuilding the level set function using the characteristic information present in these escaped marker particles. This allows the level-set method to obtain a sub-grid scale accuracy near the interface and works to counteract the well-known detrimental mass loss of the level-set method in under-resolved regions.

4.5 Resolution of multiple scales: coalescence events and film rupture

As illustrated in the first part of this work (Part 1, Lappa, 2005b), if a drop approaches another drop, the fluid in between must be "squeezed" out before the drops are sufficiently close so that the film becomes unstable to attractive forces and ruptures. Films, on the other hand, are generally believed to rupture due to short range attractive forces, once they are a few hundred Angstrom thick. Therefore, to account for the draining of films prior to rupture requires the resolution of very small length scales. This means that very dense grids are necessary to capture these aspects when front and volume tracking methods are used. Capturing the dynamics of deformable fluid-fluid interfaces in close hydrodynamic interaction with relatively coarse grids is an extremely difficult challenge for these techniques because of the critical role played by the very thin near contact lubrication zone between the interfaces. In this region, larger pressures can develop and resist coalescence. A lack of numerical resolution may result in inaccurate calculation of the lubrication pressure and in erroneous prediction of premature coalescence (Zheng et al., 2005).

It is worthwhile to stress that the problem connected to the lack of numerical resolution will be definitely overcome thanks to the progressive and continuous improvements in the performances of available computers and the consequent possibility to use more and more fine grids. A possible alternative approach can be based on the use of adaptive methods (see below).

4.6 Adaptive strategies

As outlined above, the nonlinear coupling between macro scale driving forces (e.g., gravity, Marangoni stresses), micro scale lubrication pressures (between interfaces) and nano scale van der Waals attractive forces can, in principle, affect drop and interface coalescence phenomena and, therefore, the overall topology and rheological properties of the flow. On the other hand, in many other materials science problems, analogous coupling arises between macro scale driving forces (e.g., supersaturation, diffusion, fluid motion) and micro and nano scale physics (e.g., defects, interface anisotropy and kinetics) during crystal growth, thin film deposition and alloy formation. In biology, the distribution of chemical species at the micro scale affects and is affected by cellular, tissue and organ structure and function at the meso

and macro scales (see Lappa, 2004).

Accurately capturing physical phenomena over wide ranges of scales, such as those described above, in principle can be accomplished by using robust and efficient adaptive mesh refinement algorithms. Thus, there has been much recent research in this direction.

For instance, in the so-called locally adaptive mesh refinement methods (AMR), a new mesh is constructed directly in physical space by adding or removing computational elements (or fine grids) to achieve a desired level of accuracy.

In the context of fluid interfaces, AMR has been used in front tracking (Tryggvason and coworkers, Galaktionov et al., 2000), Volume of Fluid methods (Almgren et al., 1998; Tezduyar et al., 1998; Ubbink and Issa, 1999), and level-set methods (Sussman et al., 1999b; Liao et al., 2000; Sochnikov and Efrima, 2003; Sussman, 2005).

The adaptive mesh algorithm automatically imposes a mesh element size proportional to the distance from the interface. As the interfaces deform, approach or pinch-off, the mesh dynamically maintains accurate resolution of the flow near the interface. This allows a simulation to recover the lubrication forces that resist drop approach and delay coalescence.

By means of these and similar methods, the wide range of length scales characterizing deforming fluid/fluid interfaces and thinning fluid films between drops in near-contact motion can be efficiently and accurately resolved as demonstrated by comparison to experiments, to exact solutions and to sharp-interface (boundary-integral) results (Zheng et al., 2005).

5 Multidroplet and multibubble systems: a review of existing prototype applications

Despite the outstanding capabilities of these methods, there is still a substantial lack of numerical simulations dealing with the evolution of multi-droplet (or multi-bubble) systems for finite values of the characteristic numbers obtained within the framework of VOF, front tracking or level-set methods. The following sections summarize some very recent contributions, many of which were obtained by means of multi-processor computations.

5.1 Immiscible metal alloys

5.1.1 Shear-induced mixing processes

Tang et al. (2004) have demonstrated that VOF numerical methods are capable of simulating the rheological behavior of an immiscible Zn–Pb binary alloy in shear-induced mixing processes.

The rupturing, interaction and dispersion of droplets were found to be strongly influenced by the shearing forces, viscosity ratio (viscosity of the external fluid helps resisting coalescence), turbulence, and shearing time.

5.1.2 Radial solidification process and drop Marangoni migration

More recently, Lappa (2005a) by means of VOF, focused on the controversial critical role played by drop-thermal-wake effects on the Marangoni migration mechanisms.

A container with side L= 1[cm] filled with Zinc melt, initially at T= 750 [K] and bismuth drops uniformly distributed throughout were considered. The walls of the container were supposed to be cooled with a ramping rate of 1 [K/s] under zero gravity conditions.

It was depicted in detail how all the bismuth droplets migrate towards the center of the container and how during their run some coalescence phenomena occur (i.e. they tend to agglomerate into a smaller number of larger drops, Fig. 2).

It was found that for such a case (Pr $<<$ 1 and Ma=O(100)) thermal wake effects are generally negligible and the only mechanisms playing an effective role in affecting the phase separation phenomena are Marangoni motion of the drops and the coagulation events. The temperature field, in fact, is almost diffusive (see Fig. 3). This is due to the fact that, owing to the large thermal diffusivity of these materials, temperature distortions induced by the motion of the drops are rapidly damped (they are spread over large regions).

If large Prandtl number fluids are considered (transparent and/or organic liquids), on the contrary one can expect that thermal wake effects become important. Owing to the small thermal diffusivity of these liquids, the distortion induced in the temperature field in fact should be somewhat "frozen" with respect to the times with which the drops migrate within the container.

It was also shown that, as on the ground droplets co-

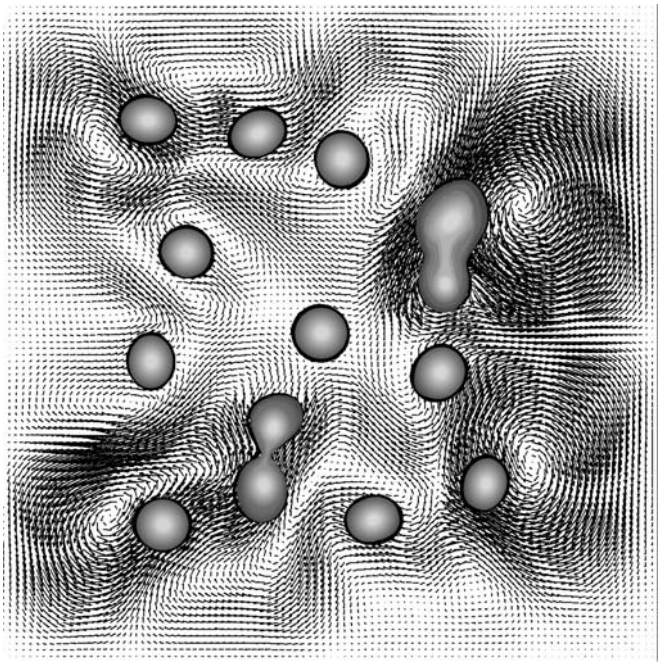

Figure 2 : Example of velocity field for Bismuth drops migrating in a container with side L= 1[cm] filled with Zinc melt, initially at T= 750 [K] with walls undergoing a cooling ramping rate of 1 [K/s] (zero gravity conditions)

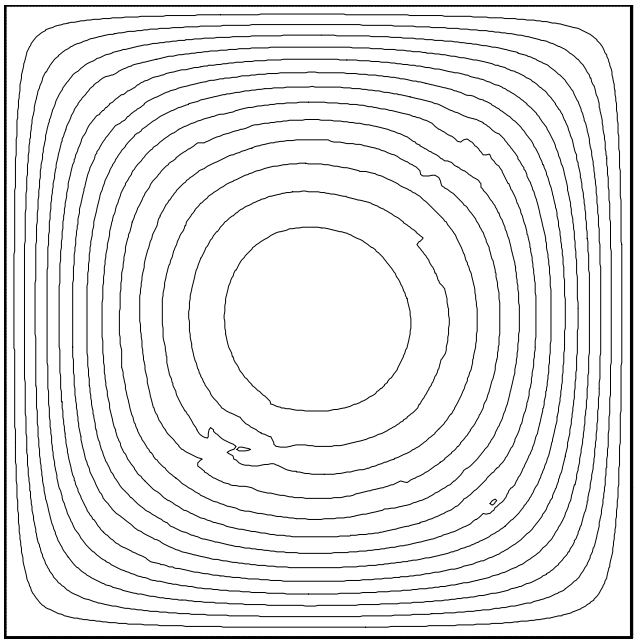

Figure 3 : Iso-contour lines of temperature distribution corresponding to Figure 2.

alescence strengthens the mechanisms leading to phase separation since heavier drops are formed with increased velocity of sedimentation (as described by Stokes' law, in fact, the sedimentation velocity of the heavy droplets increases as the square of their diameter, so big droplets settle much more rapidly than small ones), in the absence of gravity the effect is similar; drops coalescence in space leads to larger drops and this increases the velocity of Marangoni migration owing to the increase of the interface where the surface tension stresses act propelling the drop.

5.2 Bubbly flows

Bubble-driven circulation systems are used in metal processing operations such as steel making, ladle metallurgy, and the secondary refining of aluminum and copper.

This problem exhibits an outstanding theoretical kinship with that related to the evolution/dynamics of droplets in emulsions and immiscible alloys. Bubbly flows and flows with dispersed droplets, in fact, share (with the due differences) many common dynamical aspects. For these reasons, this section is devoted to a brief but very interesting review of recent results concerning this particular problem that, owing to its intrinsic nature, is very relevant within the context of this review and also represents a very good terrain for the application and validation of existing moving-boundary numerical strategies.

5.2.1 Buoyancy effects

The behavior of a gas bubble rising due to buoyancy or thermocapillarity is reasonably well understood (Clift et al., 1978; Bhaga and Weber, 1981; Sangani and Acrivos, 1983; Subramanian and Balasubramaniam, 2001).

Within the context of moving boundary methods, one of the first attempt to simulate the motion of a single bubble was the pioneering work of Ryskin and Leal (1984), who computed the steady-state shape of axisymmetric bubbles by means of a body-fitted strategy.

Like the case of droplets, however, in many practical applications relevant studies must deal with collective behaviors (many interacting bubbles). Embryonic studies along these lines are those of Sangani and Didwania (1993) and Smereka (1993) who assumed spherical bubbles moving under the effect of buoyancy forces in the limit of potential approximation.

Over recent years, however, the investigation of this problem has enjoyed a widespread use of the front tracking method introduced by Unverdi and Tryggvason (1992a).

The method was initially used to investigate the interaction of two bubbles.

The results showed that the effect of viscosity on the interaction of two bubbles is almost exactly opposite to what is predicted by potential flow theory. Two bubbles in tandem tend to attract each other and two bubbles rising side by side tend to repel each other. These phenomena, however, were only seen for bubbles in close hydrodynamic interaction whereas at larger separations the inviscid effects were found to dominate when the Reynolds number is sufficiently high.

According to these studies, therefore, two bubbles in tandem tend to repel each other if they are far apart and attract each other if they are closer and a horizontal bubble pair tend to attract each other if they are far apart and repel each other if they are close. It was also disclosed that deformation generally enhances the viscous effects. These computations provided a relatively coherent picture of the interactions of two bubbles at modest Reynolds numbers.

These studies were refined by Esmaeeli and Tryggvason (1996, 1998 and 1999) who considered many interacting rising bubbles, also referred to as "cloud" or "swarm" or "freely evolving arrays".

A freely evolving array consists of bubbles (assumed to be uniformly distributed in a certain portion of the liquid at an initial reference time) that can interact freely and can undergo different rise velocities (i.e., their spatial distribution evolves continuously). This is in contrast to the "regular array" (where the bubbles all have the same velocity and their spatial distribution essentially remains constant) used in earlier analyses by many investigators because of its relative simplicity in mathematical modeling and numerical simulation (in the limit of potential or Stokes flow).

Esmaeeli and Tryggvason (1996), by means of simulations with a few hundred two-dimensional bubbles at O(1) Reynolds numbers, elucidated that bubble motion can lead to an inverse energy cascade (where the flow structures continuously increase in size) that exhibits notable analogies with the evolution of stirred 2D turbulence; although the same interaction is not expected in three-dimensions, the simulations highlighted the crucial importance of considering large systems with many bubbles.

The Reynolds number was still relatively small (1-2) in the simulations of Esmaeeli and Tryggvason (1998), but it was increased to 20-30 in the studies of Esmaeeli and Tryggvason (1999). In both cases the bubbles were nearly spherical (Bo < 1) and most of the simulations were limited to two-dimensional flows, although a few simulations for three-dimensional systems with up to eight bubbles were included. Simulations of freely evolving arrays were compared with regular arrays and it was found that while freely evolving bubbles at low Reynolds numbers rise faster than a regular array (in agreement with Stokes flow results), at higher Reynolds numbers the trend is reversed and the freely moving bubbles rise slower.

These simulations also showed that at finite Reynolds numbers, two-bubble interactions take place by the "drafting, kissing, and tumbling" mechanism already predicted by Fortes et al. (1987) for the case of solid particles: "*For two bubbles rising in tandem, the lower one is in the wake of the one in front and is shielded from the oncoming fluid. It therefore experiences less drag but the same buoyancy force, and moves faster than the one in front. An in-line configuration of two touching bubbles is inherently unstable, and the bubbles "tumble" whereby the bottom one catches up with the top one. At the end of the tumbling the bubbles move apart*".

Bubbles first rise straight upward, but as each bubble reaches the wake of the bubble in front, the array becomes unstable and the initial configuration breaks up. In particular, bubble pairs, initially oriented vertically, tend to interact strongly, orient themselves horizontally and rise together.

Preliminary results for even higher Reynolds numbers pointed out that once the bubbles start to wobble (an oscillatory behavior occurring at sufficiently high values of the Reynolds number), the rise velocity is reduced even further, compared to the steady rise of a regular array at the same parameters. They also observed that there is an increased tendency for the bubbles to line up side-by-side (by the "drafting, kissing, and tumbling" interaction mechanism discussed before) as the rise Reynolds number increases, suggesting a monotonic trend from the nearly so-called "no preference" found by Ladd (1993) for Stokes flow, toward the strong layers (also refereed

to as "rafts") formation seen in the potential flow simulations of Sangani & Didwania (1993) and Smereka (1993).

More recently, Bunner and Tryggvason (1999a,b; 2002a,b; 2003) have introduced a parallel version of the front tracking algorithm to study the dynamics of up to two hundred three-dimensional bubbles.

In Bunner and Tryggvason (2002a), the governing parameters were selected such that the average rise Reynolds number was about 20-30 (comparable to Esmaeeli and Tryggvason, 1999, but not identical) and deformations of the bubbles were small. These simulations confirmed earlier observations of Esmaeeli & Tryggvason (1998, 1999) and in particular, showed that there is an increased tendency for the bubbles to line up side-by-side (i.e. to form rafts) as the rise Reynolds number increases.

Recent computations of Esmaeeli (2005) for the case of nearly spherical bubbles and Re=O(100) have definitely confirmed this tendency. Also, such simulations have disclosed that for such values of the Reynolds number raft formation is somewhat prevented or retarded if deformable bubbles (larger value of the Bond number, i.e. Bo > 1) are considered.

The case of deformable bubbles at intermediate values of the Reynolds number was considered by Bunner & Tryggvason (2003) who compared interactions of 27 deformable and nearly spherical bubbles at a Reynolds number of about 20 and void fraction of 6%. One of their main observations was that the deformation results in a significant modification of the bubble microstructure as a result of a reversal in the direction of the lift force.

Such a reversal effect can lead to the accumulation of the bubbles in a column. Such a phenomenon, also experimentally observed in earlier investigations by Stewart (1995) (who depicted it as a "cluster chimney"), was referred to as "streaming state" by Bunner and Tryggvason (2003); they showed that the average rise velocity of the deformable bubbles increases dramatically as a result of the formation of streams (in contrast to the formation of rafts that, as explained before, has the opposite effect).

The aforementioned recent computations of Esmaeeli (2005) in the case of deformable bubbles, however, among other things, have also proven that the deformable bubbles tendency to form columnar arrangements is suppressed at larger values of the Re number (i.e. Re=O(100)).

5.2.2 *Marangoni effects*

The investigation of bubbly flows in the framework of the freely evolving array model and of the front tracking method has not been limited to the case of gravity effects. Some works have also appeared where the possible effect of thermal Marangoni forces was elucidated.

For interaction of nearly spherical (Ca $<<$ 1) bubbles (or drops) at finite Marangoni numbers (Pr=1, Ma=O(10)), Nas & Tryggvason (1993, 2003) considered a couple of bubbles (or drops) in the case of an imposed external unidirectional temperature gradient. They disclosed that "*For two bubbles rising in tandem in an upward temperature gradient, the bubble on the top, pumps the high temperature ambient fluid from the top to the bottom. This results in an increase in the temperature of the fluid in the gap between the bubbles which leads to a decrease (respectively increase) in the temperature gradient across the top (respectively bottom) bubble. As a result, the velocity of the bubble in the wake increases while the velocity of the one on the top decreases. The bubble in the wake catches up with the top one, they nearly touch, and then, separate*".

These results (that exhibit a reversed trend with respect to those obtained by Balasubramaniam and Subramanian, 1999 in the limit of infinite Marangoni number but are in agreement with those obtained by Leshansky and Nir, 2001 in the limit of small Marangoni number) have been recently refined by Esmaeeli (2005) in the case of multi-bubble evolution.

He has shown that, if the void fraction is high enough, this thermal process (that has nothing to do with the hydrodynamic "drafting, kissing, and tumbling" mechanism that occurs in the case of buoyancy bubbly flows) leads to formation of layers (rafts) of bubbles perpendicular to the direction of the imposed temperature gradient which in turn results in a substantial decrease in the mean migration velocity of the bubbles owing to "flow blockage".

Since in the case of gravity absent, the density jump (that is of course larger in the case of a system bubble/liquid with respect to the case of droplets dispersed in a matrix) is supposed not to play a crucial role in the surface-tension driven dynamics, it is reasonable that the phenomena discussed above could partially hold in the

case of liquid/liquid systems for comparable values of the Marangoni and capillary numbers.

6 Conclusions

The problem of how best to approximate a continuous system with a discrete model has always troubled mathematicians, scientists, and engineers alike.

One of the contemporary and more complex examples of this problem is to create computer models for propagating interfaces within multiphase systems and related possible coalescence of dispersed particles (drops, bubbles). A propagating interface is a closed surface in some space that is moving under a function of local, global, and independent properties. Local properties are properties determined by local information about a curve, such as its curvature. Global properties are properties determined by the shape and positioning of the surface. Independent properties are properties not determined by the surface itself, such as an underlying flow of the surface. In the present paper a quite complete review of the state-of-the-art about these topics has been provided with emphasis on the occurrence of coalescence phenomena in systems undergoing the influence of buoyancy and/or (thermal) Marangoni forces.

An obvious justification for the long lasting (and continuing) efforts in these fields can be found in the relevance that these phenomena have in several industrial applications and many multi-material problems. However, it is rather clear that these problems have also exerted an appeal on scientists and engineers as a consequence of their intrinsic complexity. This complexity is shared with other systems in nature and constitutes a remarkable challenge for any theoretical model.

References

Adalsteinsson, D. and Sethian, J.A. (1995): A fast level set method for propagating interfaces. *J. Comput. Phys.*, vol. 118, pp. 269-277.

Almgren, A.S.; Bell, J.B.; Colella, P.; Howell L.H. and Welcome M.L. (1998): A conservative adaptive projection method for the variable density incompressible Navier-Stokes equations. *J. Comput. Phys.*, vol. 142, pp. 1-46.

Ashgriz, N. and Poo, J.Y. (1991): FLAIR: Flux line-segment model for advection and interface reconstruction. *J. Comput. Phys.*, vol. 93, pp. 449-468.

Aulisa, E.; Manservisi, S.; Scardovelli, R. and Zaleski, S., (2003a): A geometrical area-preserving Volume-of-Fluid method. *J. Comput. Phys*, vol. 192, pp. 355-364.

Aulisa, E.; Manservisi, S. and Scardovelli, R. (2003b): A mixed markers and volume-of-fluid method for the reconstruction and advection of interfaces in two-phase and free-boundary flows. *J. Comput. Phys*, vol. 188, pp. 611-639.

Balasubramaniam, R. and Subramanian, R. S. (1999): Axisymmetric thermal wake interaction of two bubbles in a uniform temperature gradient at large Reynolds and Marangoni numbers. *Phys. Fluids*, vol. 11, pp. 2856-2864.

Bazhlekov, I.B.; Anderson, P.D.; Meijer, H.E.H. (2004): Nonsingular boundary integral method for deformable drops in viscous flows. *Phys. Fluids*, vol. 16, pp. 1064-1081.

Benson, D.J. (2002): Volume of fluid interface reconstruction methods for multi-material problems. *Annu. Rev. Fluid Mech.*, vol. 55, pp. 151-165.

Bhaga, D. and Weber, M. (1981): Bubbles in viscous liquids: Shapes, wakes, and velocities. *J. Fluid Mech.*, vol. 105, pp. 61–85.

Brackbill, J.U.; Kothe, D.B.; Zemach, C. (1992): A Continuum Method for Modeling Surface Tension. *J. Comput. Phys.*, vol. 100, pp. 335-354.

Bunner, B. and Tryggvason, G. (1999a): Direct Numerical Simulations of Three-Dimensional Bubbly Flows. *Phys. Fluids*, vol. 11, pp. 1967-1969.

Bunner, B. and Tryggvason, G. (1999b): An Examination of the Flow Induced by Buoyant Bubbles. *Journal of Visualization*, vol. 2, pp. 153-158.

Bunner, B. and Tryggvason, G. (2002a): Dynamics of homogeneous bubbly flows Part 1. Rise velocity and microstructure of the bubbles. *J. Fluid Mech.*, vol. 466, pp. 17-52.

Bunner, B. and Tryggvason, G. (2002b): Dynamics of homogeneous bubbly flows Part 2. Velocity fluctuations. *J. Fluid Mech.*, vol. 466, pp. 53-84.

Bunner, B. and Tryggvason, G. (2003): Effect of bubble deformation on the properties of bubbly flows. *J. Fluid Mech.*, vol. 495, pp. 77-118.

Ccerne, G.; Petelin, S.; Tiselj, I. (2002): Numerical errors of the volume-of-fluid interface tracking algorithm, *Int. J. Numer. Methods Fluids*, vol. 38, pp. 329-350.

Chang, Y.C.; Hou, T.Y.; Merriman, B. and Osher, S. (1996): A level set formulation of eulerian interface capturing methods for incompressible fluid flows. *J. Comput. Phys.*, vol. 124, pp. 449-464.

Chen, S.; Johnson, D. and Raad, P. (1995): Velocity boundary vonditions for the simulation of free surface fluid flow. *J. Comput. Phys.*, vol. 116, pp. 262-276.

Chen, S.; Johnson, D.; Raad, P. and Fadda, D. (1997): The surface marker and micro vell method. *Int. J. for Num. Meth. in Fluids*, vol. 25, pp. 749-778.

Chopp, D.L. (1993): Computing minimal surfaces via level set curvature flow. *J. Comput. Phys.*, vol. 106, pp. 77-91.

Clift, R.; Grace, J.R.; Weber, M.E. (1978): *Bubbles, drops and particles*. Academic Press, New York, 1978.

Cristini, V.; Blawzdziewicz, J.; and Loewenberg, M. (2001): An adaptive mesh algorithm for evolving surfaces: simulations of drop breakup and coalescence. *J. Comput. Phys.*, vol. 168, pp. 445-463.

Cristini, V. and Tan, Y.C. (2004): Theory and numerical simulation of droplet dynamics in complex flows: a review. *Lab Chip*, vol. 4, pp. 257-264.

Enright, D.; Fedkiw, R.; Ferziger, J. and Mitchell, I. (2002): A hybrid particle level set method for improved interface capturing. *J. Comput. Phys.*, vol. 183, pp. 83-116.

Esmaeeli, A. (2005): Phase distribution of bubbly flows under terrestrial and microgravity conditions. *Fluid Dynam. Mater. Processing FDMP*, vol. 1, pp. 63-80.

Esmaeeli, A. and Tryggvason, G. (1996): An inverse energy cascade in two-dimensional, low reynolds number bubbly flows. *J. Fluid Mech.*, vol. 314, pp. 315-330.

Esmaeeli, A.; Tryggvason, G. (1998): Direct numerical simulations of bubbly flows. Part I–low reynolds number arrays. *J. Fluid Mech.*, vol. 377, pp. 313-345.

Esmaeeli, A.; Tryggvason, G. (1999): Direct numerical simulations of bubbly flows. Part II–moderate reynolds number arrays. *J. Fluid Mech.*, vol. 385, pp. 325-358.

Fortes, A. F.; Joseph, D. D.; and Lundgren, T. S. (1987): Nonlinear mechanics of fluidization of beds of spherical particles. *J. Fluid Mech.*, vol. 177, pp. 467-483.

Galaktionov, O.S.; Anderson, P.D.; Peters, G.W.M.; and Van de Vosse, F.N. (2000): An adaptive front tracking technique for three dimensional transient flows. *Int. J. Num. Meth. Fluids*, vol. 32, pp. 201-218.

Ginzburg, I.; Wittum, G. (2001): Two-phase flows on interface refined grids modelled with VOF, staggered finite volumes, and spline interpolants. *J. Comput. Phys.*, vol. 66, pp. 302-335.

Gueyffier, D.; Li, J. , Nadim, A.; Scardovelli, S.; Zaleski, S., (1999): Volume of Fluid interface tracking with smoothed surface stress methods for three-dimensional flows. *J. Comput. Phys.*, vol. 152, pp. 423-456

Haj-Hariri, H.; Shi, Q.; Borhan, A. (1997): Thermocapillary motion of deformable drops at finite Reynolds and Marangoni numbers. *Phys. Fluids*, vol. 9, pp. 845-855.

Harlow, F.H. and Welch, J.E. (1965): Numerical calculation of time-dependent viscous incompressible flow with free surface. *Phys. Fluids*, vol. 8, pp. 2182-2189.

Harvie, D.J.E.; Fletcher, D.F. (2000): A new volume of fluid advection algorithm: the stream scheme. *J. Comput. Phys.*, vol. 162, pp. 1-32.

Harvie, D.J.E.; Fletcher, D.F. (2001): A new volume of fluid advection algorithm: the defined donating region scheme. *Int. J. Numer. Meth. Fluids*, vol. 35, pp. 151-172..

Hirt, C.W.; Nichols, B.D. (1981a): Volume of fluid (VOF) method for the dynamics of free boundaries. *J. Comput. Phys.*, vol. 39, pp. 201-225.

Hirt, C. W. and Nichols, B. D. (1981b): A computational method for free surface hydrodynamics. *Journal of Pressure Vessel Technology*, vol. 103, pp. 136-141.

Hooper, R.; Cristini, V.; Shakya, S.; Lowengrub, J.; Macosko, C.W.; and Derby, J. J. (2001): *Modeling multiphase flows using a novel 3d adaptive remeshing algorithm. In Computational methods in multiphase flow*, Wessex Institute of Technology Press, UK, 2001.

Hogea C.S., Murray B.T., Sethian J.A. (2005): Implementation of the level set method for continuum mechanics based tumor growth models. *FDMP: Fluid Dynamics & Materials Processing*, vol. 1, no. 2, pp. 109-130.

Hou, T. Y.; Lowengrub, J. S. and Shelley, M. J. (2001): Boundary Integral Methods for Multicomponent Fluids and Multicomponent Materials. *J. Comput. Phys.*, vol. 169, pp. 302-362.

Iwasaki, T.; Nishimura, K.; Tanaka, M.; Hagiwara, Y. (2001): Direct numerical simulation of turbulent Couette flow with immiscible droplets. *Int. J. Heat Fluid*

Flow, vol. 22, pp. 332-342.

Jimènez, E.; Sussman, M.; and Ohta, M (2005): A Computational Study of Bubble Motion in Newtonian and Viscoelastic Fluids. *Fluid Dynam. Mater. Processing*, vol. 1, pp. 97-108

Kothe, D. B. (1999): Perspective on Eulerian finite volume methods for incompressible interfacial flows. in H. Kuhlmann and H. Rath, editors, *Free Surface Flows*, pages 267-331, New York, NY, 1999, Springer-Verlag.

Kothe, D.B.; Rider, W.J. (1995): *Comments on modelling interface flows with volume-of-fluid methods*. Los Alamos National Laboratory, LA-UR-94-3384, 1995.

Ladd, A.J.C. (1993): Dynamical simulations of sedimenting spheres. *Phys. Fluids*, vol. 5, pp. 299-310.

Lafaurie, B.; Nardone, C.; Scardovelli, R.; Zaleski, S. and Zanetti, G. (1994): Modelling merging and fragmentation in multiphase flows with SURFER. *J. Comput. Phys.*, vol. 113, pp. 134-147.

Lapenta, G. and Brackbill, J. (1994): Dynamic and Selective Control of the Number of Particles in Kinetic Plama Simulations. *J. Comput. Phys.*, vol. 115, pp. 213-227.

Lappa, M. (2004): *Fluids, Materials and Microgravity: Numerical techniques and insights into the physics*. Elsevier Science (Oxford, 2004): 538pp. - ISBN 00-804-4508-X.

Lappa, M. (2005a): Assessment of VOF strategies for the analysis of Marangoni Migration, Collisional Coagulation of Droplets and Thermal wake effects in Metal Alloys under Microgravity conditions. *Comput. Mat. Continua CMC*, vol. 2, pp. 51-64.

Lappa, M. (2005b): Coalescence and non-coalescence phenomena in multi-material problems and dispersed multiphase flows: Part 1, a critical review of theories. *Fluid Dynam. Mater. Processing*, present Issue.

Leshansky, A. M. and Nir, A. (2001): Thermocapillary Alignment of Gas Bubbles Induced by Convective Transport. *J. Colloid Interface Sci.*, vol. 240, pp. 544-551.

Liao, G.; Liu, F.; de la Pena, C.; Peng, D.; and Osher, S. (2000): Level-set based deformation methods for adaptive grids. *J. Comput. Phys.*, vol. 159, pp. 103-122.

Lòpez, J.; Hernàndez, Gòmez, P. and Faura, F. (2004): A Volume of Fluid method based on multidimensional advection and spline interface reconstruction. *J. Comput. Phys.*, vol. 195, pp. 718-742.

Mehdi-Nejad, V.; Mostaghimi, J.; Chandra, S. (2003): Two-fluid Heat Transfer Based on a Volume Tracking advection Algorithm. *Proceedings of 9th International Conference on Liquid Atomization and Spray Systems (ILASS-2003)*: 13-17 July, 2003, Sorrento, Italy.

Mosso, S. J.; Swartz, B. K.; Kothe, D. B.; and Ferrell, R. C., (1997): A parallel, volume-tracking algorithm for unstructured meshes. in P. Schiano, A. Ecer, J. Periaux, and N. Satofuka, editors, *Parallel Computational Fluid Dynamics: Algorithms and Results Using Advanced Computers*, pages 368-375, Capri, Italy, 1997. Elsevier Science.

Nas, S. and Tryggvason, G. (1993): Computational Investigation of the Thermal Migration of Bubbles and Drops. *in AMD 174/FED 175 Fluid Mechanics Phenomena in Microgravity, Ed. Siginer, Thompson and Trefethen*. p. 71-83, Presented at the ASME 1993 Winter Annual Meeting, ASME (1993).

Nas, S. and Tryggvason, G. (2003): Thermocapillary interaction of two bubbles or drops. *Int. J. Multiphase Flow*, vol. 29, pp. 1117-1135.

Nichols, B.D.; Hirt, C.W.; Hotchkiss, R.S. (1980): *SOLA-VOF: a solution algorithm for transient fluid flow with multiple free boundaries*. Los Alamos Scientific Laboratory Report LA-8355, 1980.

Noh, W. F. , Woodward, P. R. (1976): SLIC (simple line interface method). in *Lecture Notes in Phys.*, Vol. 59, edited by A. I. van de Vooren and P. J. Zandbergen (Springer-Verlag, Berlin/New York, 1976): pp. 330.

Osher, S. and Fedkiw, R. (2001): Level set methods: An overview and some recent results. *J. Comput. Phys.*, vol. 169, pp. 463-502.

Osher, S.; Fedkiw, R. (2002): *The Level Set Method and Dynamic Implicit Surfaces*. Springer-Verlag, New York.

Osher, S.; Sethian, J.A. (1988): Fronts propagating with curvature-dependent speed: Algorithms based on Hamilton-Jacobi formulations. *J. Comput. Phys.*, vol. 79, pp. 12-49.

Peng, D.; Merriman, B.; Osher, S.; Zhao, H.-K.; and Kang, M., (1999): A PDE-Based fast local level set method. *J. Comput. Phys.*, vol. 155, pp. 410-438.

Pilliod, J.E. Jr and Puckett, E.G. (1997): *Second-order accurate volume-of-fluid algorithms for tracking material interfaces*. Technical report, Lawrence Berkeley National Laboratory, 1997. No. LBNL-40744.

Popinet, S. and Zaleski, S. (1999): A front-tracking algorithm for accurate representation of surface tension. *Int. J. Numer. Meth. Fl.*, vol. 30, pp. 775-793.

Pozrikidis, C. (1992): *Boundary Integral and Singularity Methods for Linerarized Viscous Flow*. Cambridge University Press, Cambridge, 1992.

Puckett, E.; Almgren, A.; Bell, J.; Marcus, D. and Rider, W., (1997): A High-Order projection method for tracking fluid interfaces in variable density incompressible flows. *J. Comput. Phys.*, vol. 130, pp. 269-282.

Raad, P.; Chen, S. and Johnson, D. (1995): The introduction of micro cells to treat pressure in free surface fluid flow problems. *J. Fluids Eng.*, vol. 117, pp. 683-690.

Renardy, M. , Renardy, Y. And Li, J. (2001): Numerical simulation of moving contact line problems using a volume-of-fluid method. *J. Comput. Phys.*, vol. 171, pp. 243-263.

Renardy, Y. and Renardy, M. (2002): Prost: A parabolic reconstruction of surface tension for the volume-of-fluid method. *J. Comput. Phys*, vol. 183, pp. 400-421.

Rider, W. and Kothe, D. (1995a): Stretching and tearing interface tracking methods. *in 12th AIAA CFD Conference*, 95-1717, AIAA, 1995.

Rider, W. and Kothe, D. (1995b): A marker particle method for interface tracking. in Dwyer, H., ed., *Proceedings of the Sixth International Symposium on Computational Fluid Dynamics*, pp. 976-981, 1995.

Rider, W. J.; Kothe, D. B. (1998): Reconstructing Volume Tracking. *J. Comput. Phys.*, vol. 141, pp. 112-152.

Rudman, M. (1997a): Volume-tracking methods for interfacial flow calculations. *Int. J. Numer. Meth. Fluids*, vol. 24, pp. 671-691.

Rudman, M. (1997b): Volume-tracking methods for interfacial flow calculations. *Int. J. Numer. Meth. Fluids*, vol. 24, pp. 671-691.

Rudman, M. (1998): A volume-tracking method for incompressible multifluid flows with large density variations. *Int. J. Numer. Meth. Fluids*, vol. 28, pp. 357-378.

Ryskin, G. and Leal, L. G. (1984): Numerical Solution of Free-BoundaryProblems in Fluid Mechanics, Part 2. Buoyancy-Driven Motion of a Gas Bubble Through a Quiescent Liquid. *J. Fluid Mech.*, vol. 148, pp. 19-35.

Sangani, A. S. & Acrivos, A. (1983): Creeping flow through cubic arrays of spherical bubbles. *Int. J. Multiphase Flow*, vol. 9, pp. 181-185.

Sangani, A. S. and Didwania, A. K. (1993): Dynamic simulations of flows of bubbly liquids at large Reynolds numbers. *J. Fluid Mech.*, vol. 250, pp. 307-337.

Scardovelli, S. and Zaleski, S. (1999): Direct numerical simulation of free surface and interfacial flow. *Ann. Rev. Fluid. Mech.*, vol. 31, pp. 567-603.

Scardovelli, R. et Zaleski, S. (2000): Analytical relations connecting linear interfaces and volume fractions in rectangular grids. *J. Comput. Phys.*, vol. 164, pp. 228-237.

Scardovelli, R. and Zaleski, S. (2003): Interface Reconstruction with Least-Square Fit and Split Eulerian-Lagrangian Advection. *Int. J. Numer. Meth. Fluids*, vol. 41, pp. 251-274.

Sethian, J.A. (1995): Algorithms for Tracking Interfaces in CFD and Materials Science. *Ann. Rev. of Comput. Fluid Mech.*

Sethian, J.A. (1996): A fast marching level set method for monotonically advancing fronts. *Proc. Natl. Acad. Sci. USA*, vol. 93, pp. 1591-1595.

Sethian, J. (1999a): *Level Set Methods and Fast Marching Methods*. Cambridge University Press.

Sethian, J.A. (1999b): Fast Marching Methods. *SIAM Review*, vol. 41, pp. 199-235.

Sethian, J. (2001): Evolution, implementation, and application of Level Set and Fast Marching Methods for Advancing Fronts. *J. Comput. Phys.*, vol. 169, pp. 503-555.

Sethian, J. and Smereka, P. (2003): Level Set methods for fluid interfaces. *Annu. Rev. Fluid Mech.*, vol. 35, pp. 341-372.

Shin, S. and Juric, D. (2002): Modeling Three-Dimensional Multiphase Flow Using a Level Contour Reconstruction Method for Front Tracking without Connectivity. *J. Comput Phys.*, vol. 180, pp. 427-470.

Smereka, P. (1993): On the motion of bubbles in a periodic box. *J. Fluid Mech.*, vol. 254, pp. 79-112

Sochnikov, V. and Efrima, S. (2003): Level set calculations of the evolution of boundaries on a dynamically adaptive grid. *Int. J. Num. Meth. Eng.*, vol. 56, pp. 1913-1929.

Stewart, C.W. (1995): Bubble interaction in low-

viscosity liquids . *Int. J. Multiphase Flow*, vol. 21, pp. 1037-1046.

Subramanian, R.S.; Balasubramaniam, R. (2001): *The Motion of Bubbles and Drops in Reduced Gravity*. Cambridge University Press, Cambridge, UK.

Sussman, M. (2003): A second order coupled level set and volume-of-fluid method for computing growth and collapse of vapor bubbles. *J. Comput. Phys.*, vol. 187, pp. 110-136.

Sussman, M. (2005): A parallelized, adaptive algorithm for multiphase flows in general geometries. *International Journal of Computers and Structures*, vol. 83, pp. 435-444.

Sussman, M.; Almgren, A.; Bell, J.; Collela, P.; Howell, L.; Welcome, M. (1999b): An adaptive level set approach for incompressible two-phase flows. *J. Comput. Phys.*, vol. 148, pp. 81-124.

Sussman, M. and Fatemi, E. (1999): An efficient, interface-Preserving Level Set Redistancing Algorithm and its application to Interfacial Incompressible Fluid Flow. *SIAM J. Sci. Comput.*, vol. 20, pp. 1165-1191.

Sussman, M.; Fatemi, E.; Smereka, P. and Osher, S. (1998): An improved Level Set Method for incompressible two-Phase flow. *Computers and Fluids*, vol. 27, pp. 663-680.

Sussman, M.; Puckett, E. (2000): A coupled level set and volume-of-fluid method for computing 3D and axisymmetric incompressible two-phase flows. *J. Comput. Phys.*, vol. 162, pp. 301-337.

Sussman, M.; Smereka, P. (1997): Axisymmetric free boundary problems. *J. Fluid Mech.*, vol. 341, pp. 269-294.

Sussman, M.; Smereka, P.; Osher, S. (1994): A level set approach for computing solutions to incompressible two-phase flow. *J. Comput Physics*, vol. 114, pp. 146-159.

Tang, H.; Wrobel, L.C.; Fan, Z. (2004): Tracking of immiscible interfaces in multiple-material mixing processes. *Comput. Mat. Science*, vol. 29, pp. 103-118.

Tezduyar, T.; Aliabadi, S. and Behr, M. (1998): Enhanced-discretization interface-capturing technique for computation of unsteady flows with interfaces. *Comput. Methods Appl. Mech. Engrg.*, vol. 155, pp. 235-248.

Tomè, M. and McKee, S. (1994): GENSMAC : A computational Marker-And-Cell method for free surface flows in general domains. *J. Comput. Physics*, vol. 110, pp. 171-186.

Tornberg, A. K. and Engquist, B. (2004): Numerical approximations of singular source terms in differential equations. *J. Comput. Phys.*, vol. 200, pp. 462-488.

Torres, D. and Brackbill, J. (2000): The Point-Set Method: Front Tracking without Connectivity. *J. Comput. Phys.*, vol. 165, pp. 620-644.

Tryggvason, G.; Bunner, B.; Esmaeeli, A.; Juric, D.; Al-Rawahi, N.; Tauber, W.; Han, J.; Nas, S.;and Jan, Y.-J. (2001): A Front Tracking Method for the Computations of Multiphase Flow. *J. Comput. Phys.*, vol. 169, pp. 708-759.

Ubbink, O. and Issa, R.I. (1999): A method for capturing sharp uid interfaces on arbitrary meshes. *J. Comput. Phys.*, vol. 153, pp. 26-50.

Unverdi, O.S.; Tryggvason, G. (1992a): A front tracking method for viscous incompressible flows. *J. Comput. Phys.*, vol. 100, pp. 25-37.

Unverdi, S. O.and Tryggvason, G. (1992b): Computations of Multi-Fluid Flows. *Physica D*, vol. 60, pp. 70-83.

Williams, M. W.; Kothe, D. B.; and Puckett, E. G. (1999a): *Approximating interface topologies with applications to interface tracking algorithms*. Technical Report 99-1076, AIAA, 1999.,Presented at the 37^{th} Aerospace Sciences Meeting.

Williams, M. W.; Kothe, D. B.; and Puckett, E. G. (1999b): Convergence and accuracy of kernel-based continuum surface tension models. In W. Shyy, editor, *Fluid Dynamics at Interfaces*, pages 347-356, Boston, MA, 1999, Cambridge University Press, 1999.

Youngs, D.L. (1982): Time-dependent multi-material flow with large fluid distortion. in: K.W. Morton, M.J. Baines (Eds.): *Numerical Methods for Fluid Dynamics*, Academic Press, New York, 1982, pp. 273-285.

Youngs ,D. L. (1984): *An Interface Tracking Method for a 3D Eulerian Hydrodynamics Code*. Technical Report 44/92/35, AWRE (1984).

Zhao, H.-K.; Chan, T.; Merriman, B. and Osher, S. (1996): A Variational Level Set Approach to multiphase motion. *J. Comput. Phys.*, vol. 127, pp. 179-195.

Zhao ,H.-K.; Merriman, B.; Osher, S. and Wang, L. (1998): Capturing the Behavior of Bubbles and Drops

Using the Variational Level Set Approach. *J. Comput. Phys.*, vol. 143, pp. 495-518.

Zheng, X.; Lowengrub, J.; Anderson, A.; Cristini, V. (2005): Adaptive unstructured volume remeshing - II: Application to two- and three-dimensional level-set simulations of multiphase flow. *J. Comput. Phys.*, vol. 208, pp. 626-650.

Zinchenko, A Z.; Rother, M. A.; and Davis, R. H. (1997): A novel boundary-integral algorithm for viscous interactions of deformable drops. *Phys. Fluids*, vol. 9, pp. 1493-1515.

Zinchenko, A. Z.; Rother, M. A. and Davis, R. H. (1999): Cusping, Capture, and Breakup of Interacting Drops by a Curvatureless Boundary-integral Algorithm. *J. Fluid Mech.*, vol. 391, pp. 249-292.